Drug Metabolism and Disposition

DMD-AR-2022-000928

Supplemental data

Inhibition of cytochrome P450 2J2-mediated metabolism of rivaroxaban and arachidonic acid by ibrutinib and osimertinib

Ziteng Wang and Eric Chun Yong Chan*

Department of Pharmacy, Faculty of Science, National University of Singapore, 18 Science Drive 4, Singapore 117543

Supplemental methods

Product information for materials

Item numbers for AA and 14,15-EET from Cayman Chemical are 90010 and 50651, respectively. Catalogue numbers for ibrutinib and osimertinib from Toronto Research Chemicals are I124970 and A808075, respectively. Catalogue number for M37 (PCI-45227, dihydrodiol-ibrutinib) from MedChemExpress LLC is HY-100659. Product code for rivaroxaban from Carbosynth Ltd is FR27742. SKU for dexamethasone from Sigma-Aldrich is D2915. Product codes for 4-HBP and BHT from Thermo Fisher Scientific are p-7022362 and AC235231000, respectively. Product number for Corning UltraPool HLM 150, Mixed Gender is 452117. Product numbers for Corning Supersomes Human CYP3A4+Oxidoreductase+b5 and Human CYP2J2+Oxidoreductase+b5 are 456207 and 456264, respectively. Product numbers for Corning Gentest NADPH Regenerating System Solution A and Solution B are 451220 and 451200, respectively. Part number for HyClone FBS (South American Origin) from Cytiva is SV30160.03. Catalog numbers for DMEM/F-12, HBSS and HEPES from Gibco are 12400024, 14025076 and 15630080, respectively. Catalog number for Pierce BCA Protein Assay Kit from Thermo Fisher Scientific is 23225.

Supplemental results

Metabolite identification of ibrutinib

In both CYP2J2 and CYP3A4 incubation systems, the chromatographic peak at 2.61 min was confirmed as parent ibrutinib, with parent $[M+H]^+$ *m/z* 441 and diagnostic product ions at *m/z* 304 and 385. The peak at 2.24 min yielded the highest intensity in CYP2J2 incubation system, while it was approximately 5-fold lower in CYP3A4 samples. Its parent ion of *m/z* 457 and product ions at *m/z* 138, 304 and 320 were diagnostic of M35, a phenyl hydroxylation metabolite. Meanwhile, another peak eluting at 2.41 min with a parent *m/z* of 457 was only observed in CYP3A4 incubation system. Its MS/MS spectrum comprising product ions at *m/z* 304 and 385 was diagnostic of M39 and M40, two CYP3A4-specific metabolites with each an addition of one oxygen on the piperidine ring. The peak at 2.07 min was detected only in CYP2J2 incubation system and yielded one product ion at *m/z* 304, that was derived from parent ion at *m/z* 473. This peak corresponded to M25, a carboxylic acid metabolite, which eluted relatively earlier compared to the other previously reported metabolites (Scheers *et al.*, 2015). The peak at 2.69 min with *m/z* 459 was detected in both CYP2J2 and CYP3A4 incubation systems, yielding same diagnostic product ions at *m/z* 304 and 321 as M34, which was formed via opening of the piperidine with further reduction to a primary alcohol. M34 was also suggested as a sequential metabolite of M39 and M40 and a precursor substrate of M25. The retention time of M34 was previously reported to be shorter than the parent drug and several metabolites (Scheers *et al.*, 2015), which was inconsistent with our findings.

M37 (PCI-45227) is reported as the main circulating and active metabolite of ibrutinib (US Food and Drug Administration, 2013). It was not detected in our Q1 MS scan but yielded diagnostic product ions at *m/z* 304 and 387 in MS2 scan at low intensity in both CYP3A4 and CYP2J2 incubation systems. In subsequent metabolic stability experiments, it was detected at low levels as well (**Supplemental Fig. 4**), and the retention time was in accordance with the reference standard of M37. Our findings are expected since M37 is formed via sequential metabolism involving potential epoxide hydrolase (**Fig. 1**), which is absent in recombinant enzyme systems. We postulated that our M37 was derived from non-enzymatic hydrolysis of the unstable epoxidated ibrutinib *in vitro*.

References

Scheers E, Leclercq L, de Jong J, Bode N, Bockx M, Laenen A, Cuyckens F, Skee D, Murphy J, Sukbuntherng J, and Mannens G (2015) Absorption, Metabolism, and Excretion of Oral ^{14}C Radiolabeled Ibrutinib: An Open-Label, Phase I, Single-Dose Study in Healthy Men. *Drug Metab Dispos* **43**:289–297.

US Food and Drug Administration (2013) *Clinical Pharmacology Reviews Ibrutinib*.

Supplemental figures

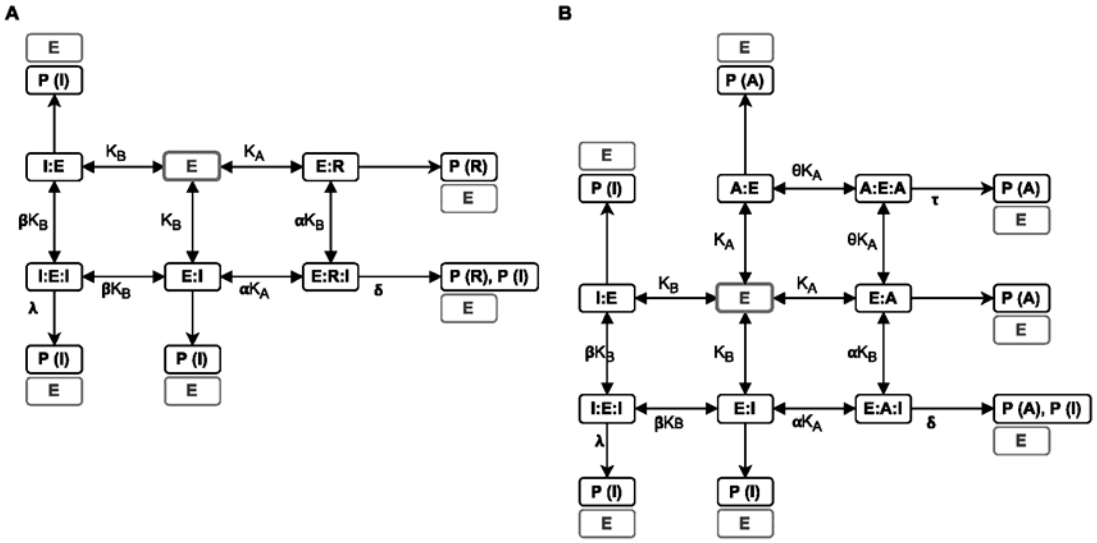

Supplemental Fig. 1. Proposed schemes of a two-site kinetic model describing CYP2J2-mediated interaction of between rivaroxaban and ibrutinib (**A**), and AA and ibrutinib (**B**), respectively. E, unbound enzyme; R, rivaroxaban; I, ibrutinib; A, AA, arachidonic acid; P, product. The corresponding equations are shown in **Equation 9**, **Equation 10**, **Equation 11** and **Equation 12**, respectively.

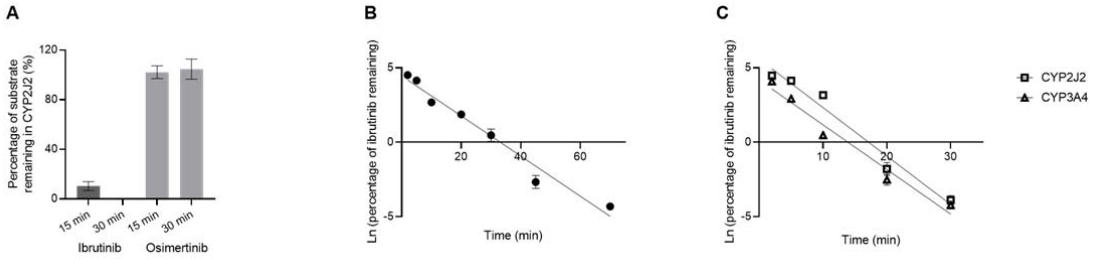

Supplemental Fig. 2. (**A**) Metabolism of ibrutinib and osimertinib by CYP2J2. Data are normalized to control samples of respective substrate without incubation. (**B**) Metabolic stability of ibrutinib in HLM incubation system. (**C**) Metabolic stability of ibrutinib in CYP2J2 (□) and CYP3A4 (△) incubation systems. Data are expressed as mean±SD. Lines in (**B**) and (**C**) represent linear regression.

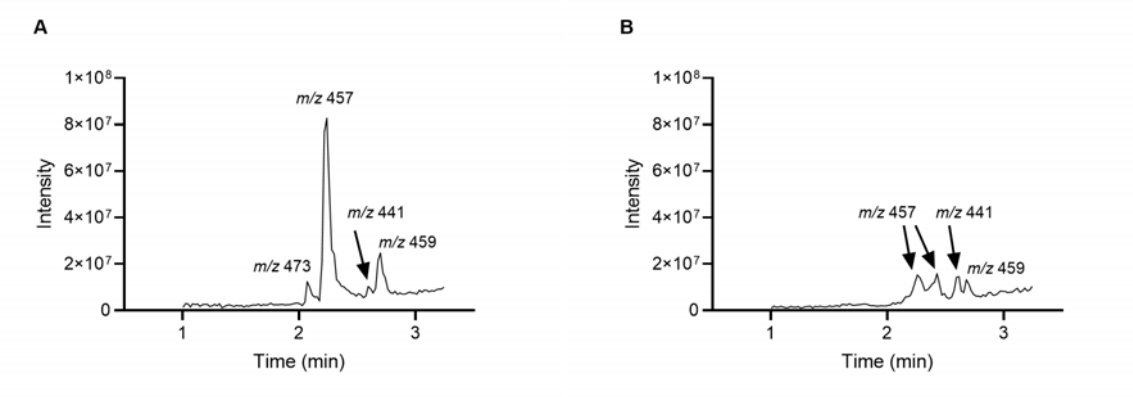

Supplemental Fig. 3. Extracted ion chromatograms of metabolites derived from recombinant (A) CYP2J2 and (B) CYP3A4 incubations.

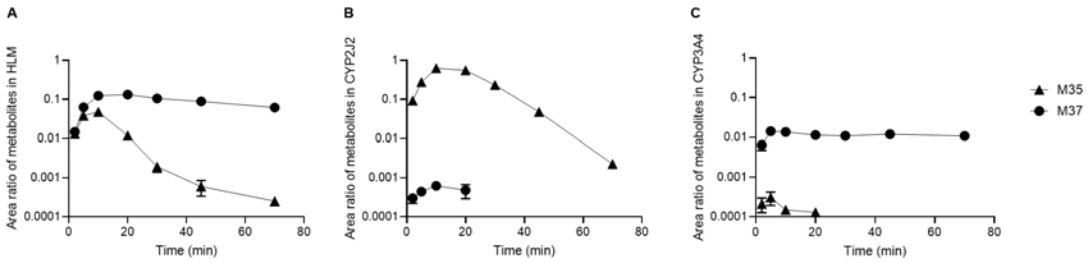

Supplemental Fig. 4. Metabolic stabilities of M35 (▲) and M37 (●) in (A) HLM, (B) CYP2J2 and (C) CYP3A4 incubation systems. Data are expressed as mean±SD.

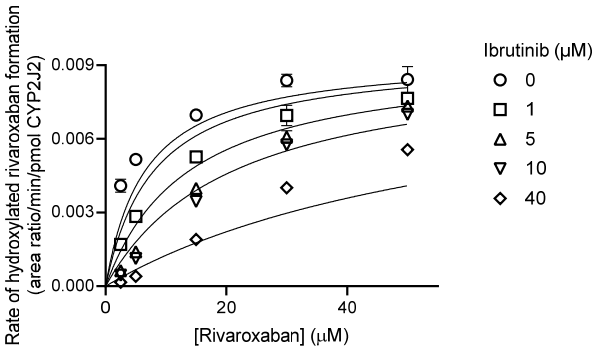

Supplemental Fig. 5. Kinetic plots of formation of rivaroxaban hydroxylation metabolite at various concentrations of ibrutinib by CYP2J2. Data are expressed as mean±SD. Line represents nonlinear regression of competitive inhibition model.

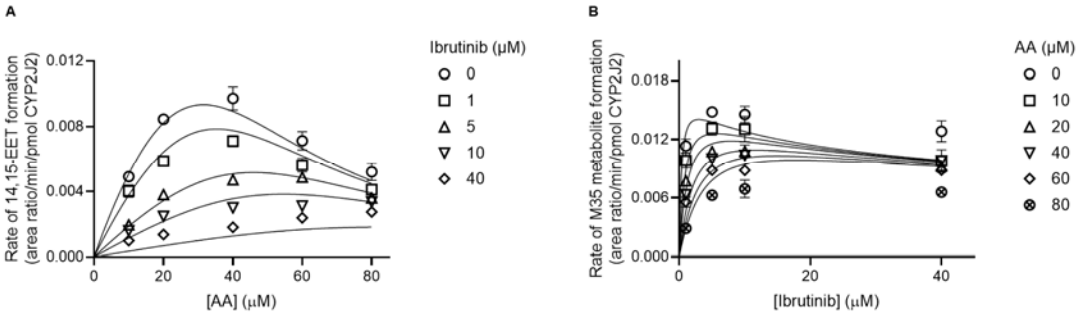

Supplemental Fig. 6. Kinetic plots of formation of 14,15-EET at various concentrations of ibrutinib (A) and formation of M35 at various concentrations of AA (B) by CYP2J2. Data are expressed as mean±SD. Line represents nonlinear regression of competitive inhibition model with substrate inhibition.

Supplemental tables

Supplemental Table 1. Incubation and sample preparation condition for reversible inhibition study of CYP2J2-mediated metabolism

Substrate	Substrate concentration (μM)	Inhibitor	Inhibitor concentration (μM)	rCYP2J2 concentration (pmol/mL)	Incubation time (min)	Quenching solution
Rivaroxaban	0, 2.5, 5, 15, 30, 50	Ibrutinib	0, 1, 5, 10, 40	10	10	ACN containing 4 μM dexamethasone (IS)
Rivaroxaban	2.5, 5, 15, 30, 50	Osimertinib	0, 2, 10, 20, 50	10	30	ACN containing 4 μM dexamethasone (IS)
Arachidonic acid	0, 10, 20, 40, 60, 80	Ibrutinib	0, 1, 5, 10, 40	20	10	ACN containing 1 μM 4-HBP (IS) and 0.001% BHT (anti-oxidant)
Arachidonic acid	10, 20, 40, 60, 80	Osimertinib	0, 2, 10, 20, 50	20	40	ACN containing 1 μM 4-HBP (IS) and 0.001% BHT (anti-oxidant)

Supplemental Table 2. Parent ion *m/z*, retention time, diagnostic product ions, relative chromatographic peak areas of ibrutinib and its metabolites after 30 min incubation of the parent drug in recombinant CYP2J2 or CYP3A4.

$[M+H]^+$ *m/z*	Retention time (min)	Diagnostic product ions	Relative peak area in CYP2J2 incubation	Relative peak area in CYP3A4 incubation	Putative identity
441	2.61	304, 385	1.98×10^7	3.70×10^7	Parent drug
457	2.24	138, 304, 320	2.29×10^8	4.00×10^7	M35
457	2.41	304, 385	N.D.	3.83×10^7	M39, M40
459	2.69	304, 320, 321	7.04×10^7	1.68×10^7	M34
473	2.07	304	4.11×10^7	N.D.	M25
475	\	304, 387	\	\	M37

N.D. = not detected

\ = no retention time and relative peak area reported for M37 at *m/z* 475 as it was detected only in MS2 scan.

Supplemental Table 3. Goodness-of-fit parameters for the fitting of various kinetic models for CYP2J2-mediated reversible inhibition

Inhibitor	Substrate	Kinetic model	AICc	Sy.x	AICc	Sy.x
			Rivaroxaban			
Osimertinib	Rivaroxaban	Competitive inhibition	-993.2	0.001284		
		Noncompetitive inhibition	-965.4	0.001545		
		Uncompetitive inhibition	-941.3	0.001815		
		Mixed mode inhibition	-990.9	0.001293		
			AA			
Osimertinib	Arachidonic acid	Competitive inhibition with substrate inhibition	-1123	0.0005358		
		Noncompetitive inhibition with substrate inhibition	-1058	0.0008259		
		Mixed mode with substrate inhibition	-1121	0.0005396		
			Rivaroxaban		*Ibrutinib*	
Ibrutinib	Rivaroxaban	Competitive inhibition	-1071	0.0007667		
		Noncompetitive inhibition	-1026	0.001031		
		Uncompetitive inhibition	-1007	0.001168		
		Mixed mode inhibition	-1068	0.0007721		
		Two-site kinetic model	-1154	0.0004273	-997	0.0009126
			AA		*Ibrutinib*	
Ibrutinib	Arachidonic acid	Competitive inhibition with substrate inhibition	-1112	0.0005764	-874.0	0.001538
		Noncompetitive inhibition with substrate inhibition	-1066	0.0007843		
		Mixed mode with substrate inhibition	-1110	0.0005805		
		Two-site kinetic model	-1118	0.0005337	-943.9	0.0008824

AICc, corrected Akaike Information Criterion; Sy.x, standard error of estimate.